Title
Relationship Between Tropical Cloud Feedback and Climatological Bias in Clouds

Journal
Geophysical Research Letters, 51(24)

ISSN
0094-8276

Authors
Thackeray, Chad W
Zelinka, Mark D
Norris, Jesse
et al.

Publication Date
2024-12-28

DOI
10.1029/2024gl111347

Relationship between tropical cloud feedback and climatological bias in clouds

Chad W. Thackeray,[1*] Mark D. Zelinka,[2] Jesse Norris,[1] Alex Hall,[1] Stephen Po-Chedley[2]

[1] Department of Atmospheric and Oceanic Sciences, University of California, Los Angeles, Los Angeles, California.
[2] Atmospheric, Earth, and Energy Division, Lawrence Livermore National Laboratory, Livermore, California.

***cwthackeray@ucla.edu**

Key Points:

- We find a relationship between tropical cloud feedback and mean-state biases in Southern Hemisphere extratropical cloud properties.
- This intermodel relationship is found to be present in three different ensembles of global climate models, a sign of robustness.
- This relationship suggests a likely tropical cloud feedback value of 0.52 ± 0.34 $W/m^2/K$, which equates to a 34% reduction in uncertainty.

Abstract

Global climate model (GCM) projections of future climate are uncertain largely due to a persistent spread in cloud feedback. This is despite efforts to reduce this model uncertainty through a variety of emergent constraints (ECs); with several studies suggesting an important role for present-day biases in clouds. Here, we use three generations of GCMs to assess the value of climatological cloud metrics for constraining uncertainty in cloud feedback. We find that shortwave cloud radiative properties across the Southern Hemisphere extratropics are most robustly correlated with tropical cloud feedback (TCF). Using this relationship in conjunction with observations, we produce an EC that yields a TCF value of 0.52 ± 0.34 $W/m^2/K$, which equates to a 34% reduction in uncertainty. Thus, we show that climatological cloud properties can be used to reduce uncertainty in how clouds will respond to future warming.

Plain Language Summary

Different global climate models exhibit large variability in how clouds across the tropics will respond to future warming. This is largely due to the complexity and diversity of responses that differing cloud types may experience under warming. A long-term goal of the community has been to narrow this disagreement between different models. Over the past 15 years, several studies have proposed ways in which the variability in future cloud changes might be related to errors in how these models represent present-day properties. Here, we use three collections of models to show that variability in tropical cloud changes is closely tied to shortwave cloud radiative properties across the Southern Ocean. We then use this intermodel relationship along with observations to produce a best estimate of cloud feedback across the tropics.

1. Introduction

Global climate models (GCMs) have long disagreed about how clouds will respond to future warming, as exemplified by a large and persistent intermodel spread in cloud feedback (Cess et al. 1990; Bony and Dufresne, 2005; Bony et al. 2006; Webb et al. 2013; Zelinka et al. 2020). Given that cloud feedback is the largest source of uncertainty for model estimates of equilibrium climate sensitivity (ECS) (Caldwell et al. 2016; Sherwood et al. 2020), there has been a major emphasis on determining which projected cloud changes are most likely. Emergent constraints (ECs) are a popular approach to tackling this problem as they use intermodel relationships between current and future climate metrics in conjunction with observations to narrow uncertainty (Klein and Hall 2015; Williamson et al. 2021). Past studies have suggested that both observable cloud variations with temperature change (Qu et al. 2014; Zhai et al. 2015; Zhou et al. 2015; Brient and Schneider 2016; Jiang et al. 2023) and climatological biases in cloud or radiative properties (Williams and Tselioudis 2007; Volodin 2008; Trenberth and Fasullo 2010; Klein et al. 2013; Brient et al. 2016; Lipat et al. 2017; Siler et al. 2018) might directly affect cloud feedback, and thus ECS.

Here we focus on the latter hypothesis, and briefly discuss two proposed mean-state biases of relevance to global cloud feedback (GCF). Building off Volodin (2008), Siler et al. (2018) use the Fifth Coupled Model Intercomparison Project (CMIP5) to find a strong relationship between GCF/ECS and the difference in cloud contributions to albedo between regions of warm versus cool (separated by 23.5°C isotherm) sea surface temperatures (SSTs) (derived as a projection of each model's albedo climatology onto the albedo-GCF correlation map). They also show that the contrast in top-of-atmosphere (TOA) shortwave cloud radiative effect (SWCRE) between these two regions is a strong predictor of GCF. This study indicates that the present-day distribution of clouds could inform future cloud changes through cloud albedo's dependence on SSTs and the future expansion of warm SSTs. However, the physical reasoning behind the constraint has been questioned (Caldwell et al. 2018).

Another example suggests that the present-day TOA energy balance across the Southern Hemisphere (SH) is strongly tied to ECS in CMIP3 (Trenberth and Fasullo 2010). They argue that GCMs with less cloud cover (and thus a more positive TOA radiative imbalance) across the Southern Ocean might have greater potential for increased cloud cover in a warming climate. However, this relationship was negligible in CMIP5 (Grise et al., 2015). Moreover, the CMIP3 relationship was found to be driven by a subset of GCMs characterized by unrealistically bright present-day clouds in the SH subtropics. Instead, Grise et al. (2015) pointed to present-day cloud and net radiation biases in subtropical stratocumulus-to-cumulus transition regions as important for explaining ECS variability.

This exemplifies a common issue encountered with proposed constraints on ECS and GCF: failed "out-of-sample" testing (Caldwell et al. 2018; Schlund et al. 2020), where a proposed relationship is not found in a different ensemble (Hall et al. 2019). Given these difficulties, several recent efforts have targeted specific cloud regimes (Qu et al. 2015; Terai et al. 2016; Myers and Norris, 2016; McCoy et al. 2020; Myers et al. 2021; Hirota et al. 2021) or regions (Lutsko et al. 2021; Wall et al. 2022) with the prevailing thought being that it is unlikely for a single current climate metric to robustly explain uncertainty in the highly complex ECS or GCF (Sherwood et al. 2020).

Here, we use three generations of GCMs to assess the potential value of climatological cloud biases for constraining regional cloud feedbacks. We primarily focus on metrics that have been shown to strongly correlate with either ECS or GCF in prior studies as these relationships likely exploit some regional relationship, which happens to control intermodel spread.

2. Data and Methods

2.1 Climate Models

We use output from a collection of 55 GCMs from the three most recent phases of CMIP (CMIP3, CMIP5, CMIP6) (Meehl et al. 2007; Taylor et al. 2012; Eyring et al. 2016) (Tables S1-

3). Model data comes from the first realization of the pre-industrial control (piControl), AMIP, and abrupt-4xCO_2 experiments. The latter is a 150-year simulation in which the atmospheric CO_2 is instantaneously quadrupled from pre-industrial levels and then held fixed. The abrupt forcing experiment was not run for CMIP3, so we rely on the 1pctCO2 experiment instead. We use ECS values from Zelinka et al. (2020) for CMIP5/6 and model development papers for CMIP3.

2.2 Cloud Metrics

Cloud feedback is calculated following Zelinka et al. (2020) for CMIP5 and CMIP6 models. First, annual anomalies are computed using the abrupt-4xCO2 experiment with respect to contemporaneous 21-year running means from piControl to account for possible model drift (Caldwell et al. 2016). Cloud feedback is then derived by adjusting the TOA CRE (clear-sky minus all-sky upwelling flux) feedback for non-cloud effects (Soden et al. 2008; Shell et al., 2008). For CMIP3, we calculate the SWCRE feedback by first computing anomalies of SWCRE averaged over years 60-80 from the 1pctCO2 experiment (surrounding the point when atmospheric CO_2 has doubled) relative to the same years of piControl. These anomalies are then normalized by the change in global and annual mean surface air temperature. Because these CMIP3 results are not directly comparable to those of CMIP5/6, we only consider the latter when building an EC on cloud feedback.

We also calculate several climatological cloud metrics. All climatological metrics used throughout are calculated as 30-year means derived from each piControl simulation (years 100-130 or the last 30 years if less than 130 years are available) and remapped to a common 2.5°x2.0° grid. (Note that for AMIP results, we use the entire simulation period for each ensemble.) The metrics evaluated here include SW and LW CRE at both the surface (SFC) and TOA, total cloud cover (CLT), and condensed water path (CWP). TOA CRE is defined as the clear- minus all-sky upwelling radiative flux at the TOA. CRE at the SFC is defined by subtracting the all- minus clear-sky surface upwelling flux from the all- minus clear-sky surface downwelling flux. We will primarily focus on SFC SWCRE rather than TOA because it exhibits a slightly better correlation with cloud feedback, but these terms are strongly correlated across models (r=0.96). We assess CLT because many GCMs do not provide the appropriate variables for cloud fraction at differing levels of the atmosphere.

Lastly, we break down simulated SWCRE into contributions from cloud albedo and cloud amount to interpret model biases. TOA SWCRE can be derived from the clear- and all-sky SW radiative fluxes:

$$SWCRE = SW_{clr} - SW_{all} = CLT * (SW_{clr} - SW_{ov}) \quad (1)$$

where SW_{ov} is the overcast SW radiative flux, which can be computed from (2).

$$SW_{all} = CLT * SW_{ov} + (1\text{-}CLT) * SW_{clr} \quad (2)$$

The difference in SWCRE either between two groups or with respect to a given GCM's ensemble mean can then be decomposed into two components:

$$\Delta SWCRE = \Delta CLT * (SW_{clr} - SW_{ov}) + CLT * \Delta(SW_{clr} - SW_{ov}) \quad (3)$$

The first term (cloud amount contribution) is derived by holding the radiation contrast term (essentially cloud albedo) constant, while the second term is derived from holding the cloud fraction constant.

2.3 Observational Data

An observational estimate of climatological SFC SWCRE is computed from the Clouds and the Earth's Radiant Energy System (CERES) dataset (Kato et al. 2018). Since surface products from CERES are more uncertain than their TOA counterparts (Loeb et al. 2018), we also calculate SFC SWCRE from ECMWF Reanalysis version 5 (ERA5; Hersbach et al. 2020, 2023). We use data from 2001-2021 to derive these climatological means. The average of these two estimates is used throughout. Since the datasets exhibit such good agreement in extratropical SFC SWCRE, we also calculate annual average SFC SWCRE to quantify interannual variability in this metric. The standard deviation (or the more conservative range) of these annual values is treated as observational uncertainty.

2.4 Constraint Methods

Constrained estimates of cloud feedback are computed using the hierarchical EC framework of Bowman et al. (2018). This method accounts for the correlation strength, observational uncertainty, and the signal-to-noise ratio between observational and GCM uncertainty. The constrained 95% prediction interval is compared to the unconstrained 95% prediction interval to measure an EC's value at reducing uncertainty. We also use the EC correlation decomposition method of Caldwell et al. (2018) to better understand the geographical breakdown of the relationship between SH extratropical SFC SWCRE and GCF. We adapt their equation 6 as follows:

$$\mathrm{corr}(X, GCF) = \sigma(CF_{local})/\sigma(GCF) * \mathrm{corr}(X, CF_{local}) \quad (4)$$

The decomposition value at each grid cell is the product of the cross-model correlation between a current climate metric (denoted by X) and the local cloud feedback (CF_{local}) (Fig. S1a-c), and the ratio of CF_{local} variability (σ; sampled across the ensemble) to GCF variability (Fig. S1d-f).

3. Results

3.1 Relevance of Climatological SFC SWCRE to Cloud Feedback

We first assess how the gradient in climatological SFC SWCRE between warm and cool SST regions (inspired by Siler et al. 2018) correlates with zonal-mean cloud feedback across three CMIP generations (Fig. 1a). It is important to gauge EC robustness using multiple ensembles because a relationship can appear in a single ensemble by chance (Caldwell et al. 2014) and large changes can occur from one ensemble to the next (Schlund et al. 2020; Text S1; Fig. S2). Strong correlations are evident over 40°S-30°N for CMIP5, which is expected since this EC was developed on CMIP5. These latitudes also happen to coincide with regions where zonal-mean cloud feedback is strongly correlated (r>0.7) with GCF (illustrated by bars along the x-axis of Fig. 1a). Because of this, the gradient metric is strongly correlated with both the tropical cloud feedback (TCF; defined as 30°S-30°N; r=0.80) and GCF (r=0.76). However, we find substantially weaker correlations in both CMIP3 (r=-0.15 for TCF, -0.29 for GCF) and CMIP6 (r=0.23 for TCF, 0.24 for GCF). Cross-model correlation maps show that this weakening is tied to a less positive, or even negative, correlation between SWCRE across warm SST areas and TCF in CMIP3 and CMIP6 (Fig. 2a-c). Moreover, in CMIP6, there is a southward shift in which latitudes are driving variability in GCF, whereby 40-60°S plays a more important role (Fig. 1a). These latitudes are also more important for ECS variability in CMIP6 (Lutsko et al. 2021).

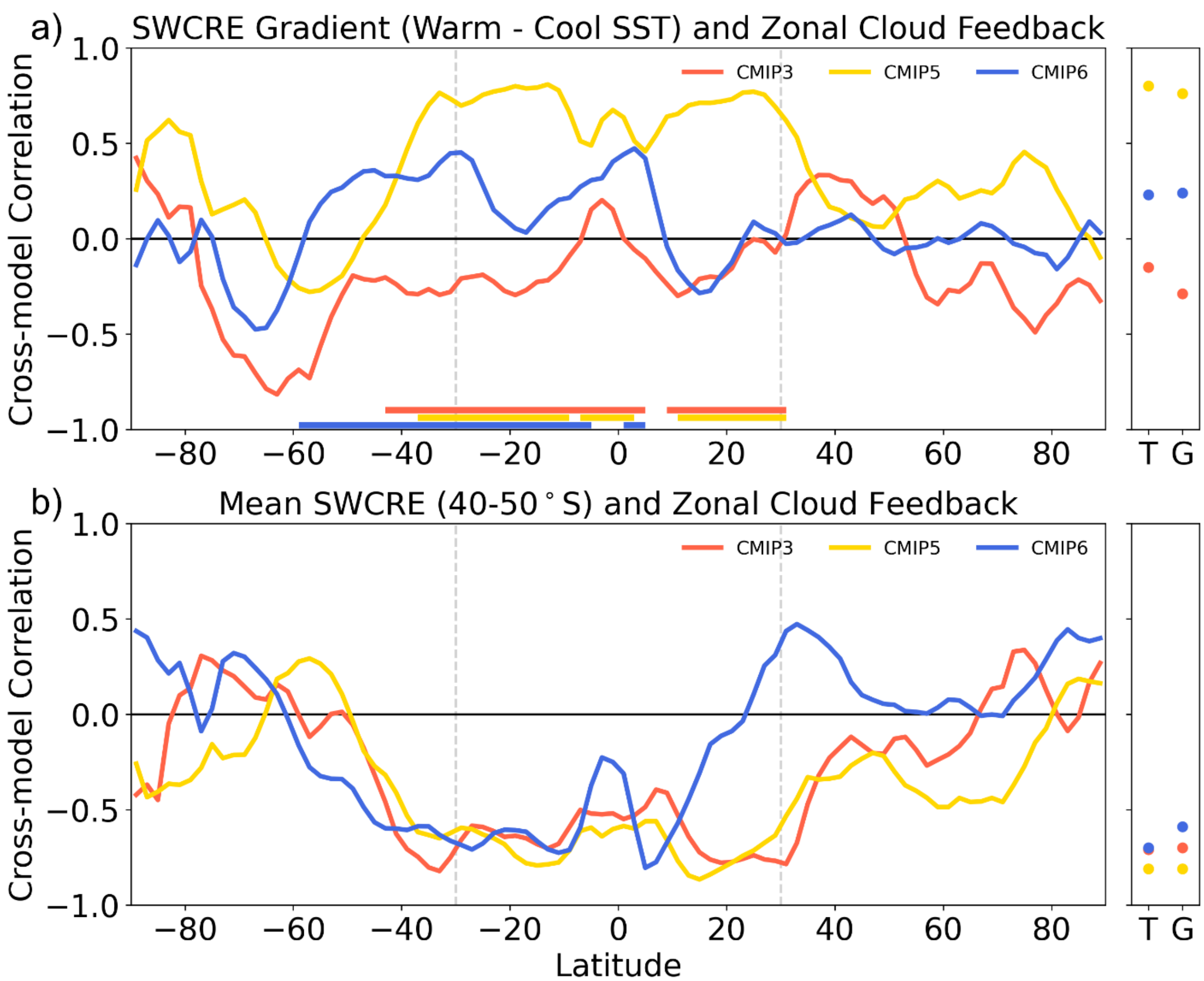

Fig. 1. Cross-model correlation between zonal-mean cloud feedback and (a) the gradient in SFC SWCRE between areas of warm and cool SSTs inspired by Siler et al (2018), (b) the mean SFC SWCRE over 40-50°S. Individual colored lines represent the results for each of the CMIPs. Latitudes where zonal-mean cloud feedback is strongly

correlated ($r>0.7$) with GCF are illustrated on panel a by horizontal bars along the x-axis. Cross-model correlations between these metrics and TCF/GCF are also shown on the right panel of each plot as colored dots.

Building off prior work which suggests potential connections between SH radiative fluxes to GCF and ECS (Trenberth and Fasullo 2010; Grise et al. 2015), we also evaluate the relevance of SWCRE across the SH to zonal-mean cloud feedback. We find that 40-50°S SFC SWCRE is strongly tied to cloud feedback across much of the 40°S-20°N range in all three ensembles (Fig. 1b). This manifests as a strong negative correlation with TCF, with correlations ranging from -0.70 in CMIP6 to -0.81 in CMIP5. Because these latitudes tend to control a substantial portion of intermodel variability in GCF, there is also a strong correlation with GCF in CMIP3 ($r=-0.70$) and CMIP5 ($r=-0.81$). The CMIP6 result is slightly weaker ($r=-0.59$) given a greater role for the SH mid-latitudes in controlling GCF and less negative correlations at the equator and north of 15°N. Weaker equatorial correlations stem from two anomalous GCMs, while the decline polewards of 15°N is driven by weak feedbacks in the CESM2 models (Fig. S3). (Note that similar analysis was performed for a variety of other metrics (LWCRE, TOA SWCRE, CLT, CWP, and TOA albedo; Fig. S4) and latitude bands (Fig. S5), but this is not discussed for brevity).

Given the robustness of the 40-50°S SFC SWCRE relationships, this will be our focus going forward. Cross-model correlation maps emphasize that a strong anti-correlation between TCF and SFC SWCRE over mid-latitude ocean basins is the main persistent feature of this relationship across generations (Fig. 2a-c). This relationship is particularly robust in the SH, where climatological cloud cover is very large (Grise et al. 2015; Kay et al. 2016). We can better understand the relationship between 40-50°S SFC SWCRE and GCF using the correlation decomposition framework of Caldwell et al. (2018). This method dissects cross-model correlations to quantify the contribution of a specific region (see Methods). It considers both the cross-model correlation between 40-50°S SFC SWCRE and the local cloud feedback (Fig. S1a-c), and the ratio of local cloud feedback variability to GCF variability (Fig. S1d-f). The decomposition shows large-scale consistency across model generations: larger climatological 40-

50°S SWCRE corresponds to greater local cloud feedback throughout the tropics (Fig. 2d-f). Regions with important low cloud feedback off the west coasts of South America, Africa, and Australia contribute to the negative correlation, but the magnitude and precise locations vary by ensemble.

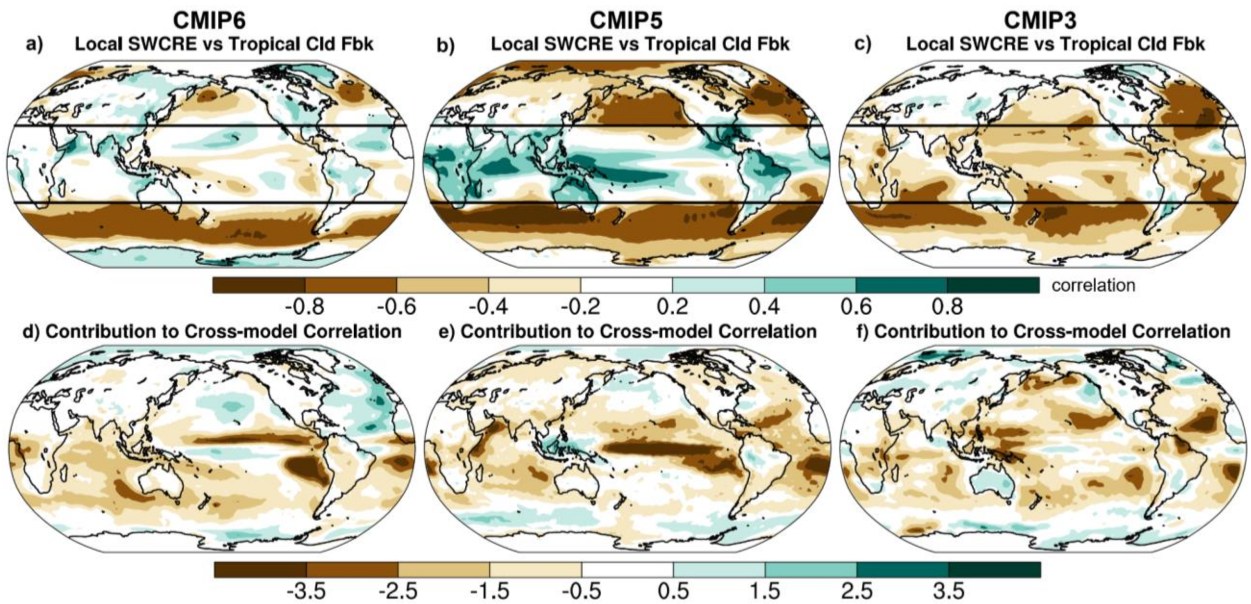

Fig. 2. Cross-model correlation maps between local SFC SWCRE and TCF for (a) CMIP6 (b) CMIP5 (c) CMIP3. Regionally decomposed cross-model correlation (see Methods) for the relationship between 40-50°S SFC SWCRE and GCF following Caldwell et al. (2018) for (d) CMIP6 (e) CMIP5 (f) CMIP3. The local contribution values can be spatially averaged to obtain the correlation shown in Figure 2b. Solid black lines denote the tropical region (30°S-30°N).

3.2 Emergent Constraint on Tropical Cloud Feedback

Given the robustness of this relationship, we build an EC on TCF. In Figure 3a we scatter climatological SFC SWCRE averaged across 40-50°S against the TCF. (Note that these climatological values are very similar in magnitude and strongly correlated with those derived from historical and AMIP simulations). For reference, we also show the relationship with GCF (Fig. 3c). Observations from CERES and ERA5 over 2001-2021 are used in conjunction with this relationship to form the EC. We derive an estimate of observational uncertainty from interannual variability. The observed estimate (-73.5 ± 0.8 W/m^2; [66% confidence interval]) suggests that GCMs tend to be negatively biased when it comes to SH mid-latitude SFC SWCRE (average of all GCMs: -76.1 ± 11.6 W/m^2). CMIP3 is the most consistently negatively biased (-79.9 ± 9.9 W/m^2), signaling that some progress has been made. However, because the CMIP3 cloud feedback values are not derived in the same way as for CMIP5/6 (see Methods), we exclude this data when building the EC. Given the similar slopes for each ensemble, we only report results for a combined ensemble of CMIP5 and CMIP6 (individual ensemble results are in Text S2).

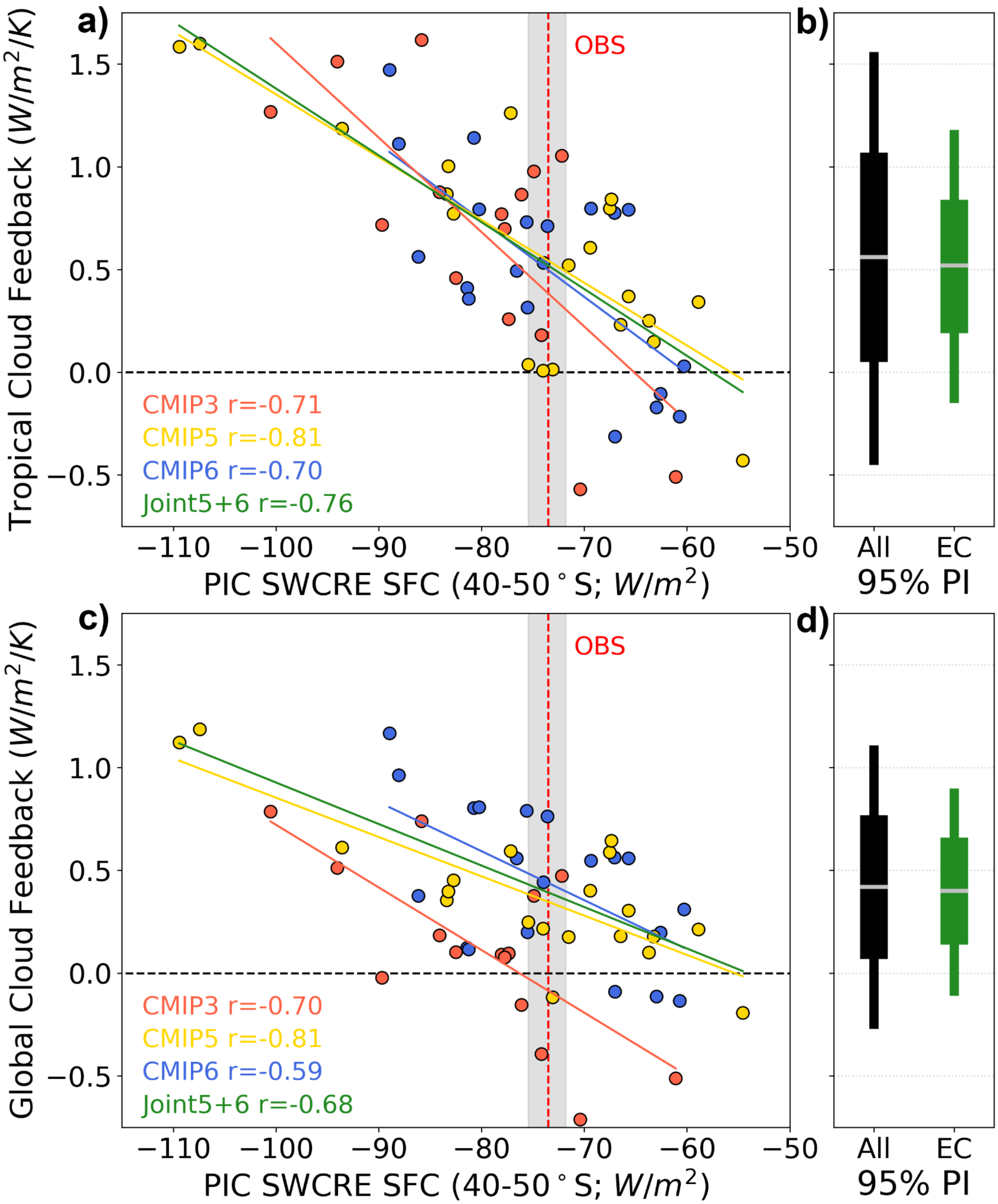

Fig. 3. Scatterplot of climatological SFC SWCRE averaged over 40-50°S versus (a) TCF, (c) GCF where each point represents a different GCM. The vertical dashed red line represents an observed estimate from observations (CERES, ERA5) while grey shading denotes the range in annual mean values, which is used in the derivation of the EC (see Methods). (b) 95% prediction interval of TCF for the unconstrained CMIP5/6 ensemble (black) and the EC (green). (d) same as b but for the GCF. The horizontal grey dash denotes the central estimate for each dataset, while the wider portion of the bar shows the 66% prediction interval.

The EC yields a TCF value of 0.52 ± 0.34 $W/m^2/K$, which represents a 34% reduction in the likely range of TCF (Fig. 3b). We use a conservative 95% prediction interval (PI) derived from the hierarchical EC framework (Bowman et al. 2018) to measure the uncertainty reduction (see Methods). The central estimate of TCF is slightly reduced from the unconstrained ensemble (0.56 ± 0.51 $W/m^2/K$). This constraint is also slightly weaker than a prior estimate using monthly and annual CRE-based tropical cloud variability metrics to constrain TCF (90% confidence interval of -0.22-1.39 $W/m^2/K$; Lutsko et al. 2021). For reference, we also show the resulting EC for GCF (Fig. 3d), which exists because of the key role that the tropics play in driving GCF spread (Fig. S1d-f). This constraint suggests a GCF value of 0.40 ± 0.26 $W/m^2/K$, which represents a 26% reduction in the likely range compared to the unconstrained ensemble (0.42 ± 0.35 $W/m^2/K$). Our constrained GCF estimate also agrees well with the two most notable community assessments in recent years (Sherwood et al. 2020: 0.45 ± 0.33 $W/m^2/K$; Forster et al. 2021: 0.42 ± 0.30 $W/m^2/K$).

3.3 Investigating Drivers of Model Spread

To better understand the relationship between 40–50°S SFC SWCRE and TCF, we group GCMs by their 40–50°S SFC SWCRE (ten highest and ten lowest across CMIP3/5/6; Tables S1-3) and assess differences in the subsequent group averages. As per the emergent relationship, the Group 1 models (more negative SFC SWCRE) exhibit much stronger cloud feedback than their Group 2 counterparts (less negative SFC SWCRE) (Fig. 4a). In terms of GCF, their group means are 0.74 $W/m^2/K$ and 0.04 $W/m^2/K$, respectively. This discrepancy stems from the tropics, where the difference between group means is even larger (1.26 W/m^2/K, -0.03 W/m^2/K). This contributes to large differences in ECS as well (4.35 vs 2.85K). It has been hypothesized that high ECS models simulate too many stratocumulus clouds in regions dominated by cumulus clouds, thus producing a stronger response of low clouds to warming (Cesena and Del Genio, 2021). However, CMIP output does not let us assess these cloud types.

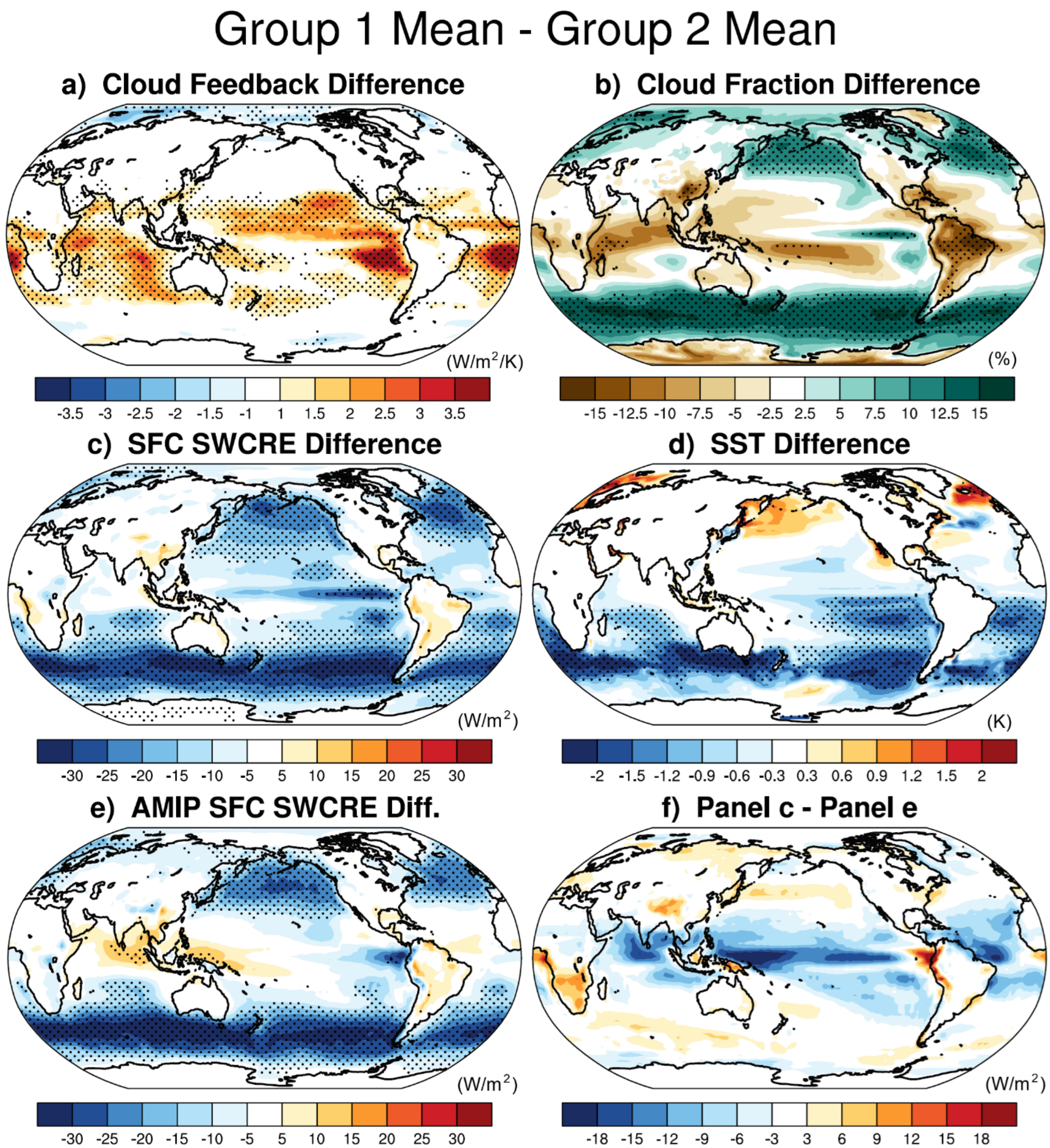

Fig. 4. Maps of the difference in (a) cloud feedback, (b) climatological total cloud fraction, (c) climatological SFC SWCRE, and (d) climatological sea surface temperatures between two groups of GCMs defined based on their

climatological 40-50°S SFC SWCRE. Group 1 models have a more negative SFC SWCRE than group 2. (e) same as panel c but derived from AMIP simulations, (f) influence of coupling on the SFC SWCRE difference between the two groups. Stippling indicates areas of statistical significance determined using a t-test ($p < 0.05$).

We find that Group 1 models consistently have greater CLT across extratropical oceans (Fig. 4b), which is surprising given that Group 2 contains more CMIP6 models (4/10 vs. 3/10), and that CMIP6 has systematically increased CLT relative to CMIP5 (Fig. S2). Moreover, while Group 1 models by definition have more negative extratropical SFC SWCRE, this discrepancy also extends to parts of the tropical oceans (Fig. 4c), particularly where cloud feedback differences are large (Fig. 4a). Group 1 contains more CMIP3 models, which exhibit unrealistically bright clouds in the SH subtropics, but similar results hold when CMIP3 is excluded (Fig. S6). SWCRE differences largely coincide with Group 1 models exhibiting cooler climatological sea surface temperatures (SSTs) across much of the SH and particularly the southeast Pacific (Fig. 4d), conditions that favor greater low-level cloud development (Mechoso et al. 2016). Since similar SFC SWCRE differences are also apparent in AMIP simulations (Fig. 4e), these cooler SSTs are likely driven partly by more negative SFC SWCRE, rather than vice versa. Fully coupled simulations even enhance SFC SWCRE differences in tropical low-cloud regions (Fig. 4f). These results agree with past work, which shows that through radiative perturbation experiments, extratropical energy biases can influence mean-state tropical SSTs and clouds (Mechoso et al. 2016; Kang et al. 2020; Kang et al. 2023).

3.4 Discussion of Mechanisms

The physical mechanisms driving the relationship between climatological SH extratropical SFC SWCRE and TCF are complex, but we offer some speculation for why this relationship exists. As suggested above, SH extratropical SWCRE affects tropical low clouds through a teleconnection likely via the southeast Pacific. Kim et al. (2022) hypothesize that SH extratropical cooling propagates into the subtropics and is advected further equatorward by climatological winds. This cooling is then enhanced by a series of processes including the wind-evaporation-SST feedback, stratocumulus cloud feedback, and coastal upwelling. We find that GCMs with more negative 40-50°S SWCRE tend to exhibit more negative SWCRE and cooler SSTs across tropical low cloud areas (Fig. 4). These cooler conditions likely help promote greater, more reflective climatological low clouds in the tropics. In fact, the presence of brighter clouds in Group 1 models becomes evident across most latitudes when the SWCRE difference between Groups 1 and 2 is decomposed into contributions from cloud amount and albedo (Fig. S7; see Methods). Therefore, when these brighter clouds are subjected to future warming, which promotes the loss of low clouds, the GCM produces a stronger cloud feedback (Fig. 4a). Notably, the Group 1 models also feature a slightly stronger reduction in tropical CLT (-4.3% compared to -1.3% in Group 2).

In contrast to the SH extratropics, mean-state tropical cloud properties are subject to a variety of influences that mask any relationship with TCF (Fig. 2a-c). For instance, the cloud brightness differences noted previously are counteracted by greater cloud amount across the tropics in Group 2 models. This contrasts with the SH, where cloud amount differences enhance the cloud brightness discrepancy. Moreover, this disconnect between SFC SWCRE and cloud feedback locally is likely exacerbated by large intermodel differences in tropical cloud coverage (e.g., in location and extent; Fig. S8) as CLT and SWCRE exhibit their best agreement in low cloud areas (Fig. S8e). Lastly, the idea that SH extratropical cloud properties are relevant to tropical clouds is supported by a moderate correlation between 40-50°S SWCRE in CMIP5-6 with two climatological cloud metrics computed across the tropics (deseasonalized monthly and annual CRE sensitivities) from Lutsko et al. (2021) (Fig. S9).

4. Conclusions

Using climatological biases for ECs is a potentially promising avenue for research as it gives modeling centers a relatively easy target metric to monitor during development stages. Here, we use three ensembles of GCMs to explore the potential of using climatological biases in clouds for constraining regional cloud feedback. We find the greatest value in climatological SFC SWCRE across the SH mid-latitudes (40-50°S), which is strongly tied ($|r|\geq 0.7$) to TCF in all generations. Using this relationship in conjunction with observations, we produce an EC on TCF, which suggests a TCF of 0.52 ± 0.34 $W/m^2/K$, compared to the unconstrained estimate of 0.56 ± 0.51 $W/m^2/K$. This suggests that the model mean is slightly too strong, while also representing a 34% reduction in model uncertainty. Given the importance of the tropics to GCF, 40-50°S SFC SWCRE can also be used to infer a GCF value of 0.40 ± 0.26 $W/m^2/K$, which agrees well with two notable community assessments (Sherwood et al. 2020; Forster et al. 2021).

Past research identified various metrics as potentially relevant to variability in TCF/GCF. This includes parametric differences in extratropical mixed phase cloud partitioning (McCoy et al. 2016). While we find this metric (known as T5050: temperature where ice and liquid phases are equal) to be only weakly correlated with 40-50°S SFC SWCRE across a set of 23 CMIP5/6 models ($r=-0.16$), it is possible that there are other unknown GCM tuning dynamics at play here. Our results also suggest that the warm-cold SWCRE gradient is not useful beyond CMIP5, potentially at odds with prior work (see Text S3). As past studies have noted, finding these relationships is the first step to understanding them, but healthy skepticism should be maintained about this EC until it is better understood (Caldwell et al. 2014; Klein and Hall, 2015). Future work should seek to better understand mechanisms and the sources of model bias in SFC SWCRE across the SH extratropics.

Acknowledgements

We acknowledge funding from the Regional and Global Model Analysis Program for the Office of Science of the U.S. Department of Energy through the Program for Climate Model Diagnosis and Intercomparison (PCMDI). The work of M. D. Zelinka and S. Po-Chedley was performed under the auspices of the U.S. Department of Energy by Lawrence Livermore National Laboratory under contract DE-AC52-07NA27344. We thank the World Climate Research Programme's Working Group on Coupled Modeling and the individual modeling groups for their roles in making CMIP data available. We also thank the two reviewers for their constructive feedback.

Open Research

All data used in this study is publicly available. The CMIP output (models listed in Tables S1-S3) is available from the Earth System Grid Federation (https://aims2.llnl.gov/search). CERES data is available from: https://ceres.larc.nasa.gov/data/. Data from ERA5 (Hersbach et al. 2023) were also used in the creation of this manuscript. The code relating to this study (Thackeray et al. 2024) is available from: https://github.com/cwthackeray/GRL-clouds.

References

Bony, S., & Dufresne, J. L. (2005). Marine boundary layer clouds at the heart of tropical cloud feedback uncertainties in climate models. *Geophysical Research Letters*, 32(20), 1–4. https://doi.org/10.1029/2005GL023851

Bony, S., Colman, R., Kattsov, V. M., Allan, R. P., Bretherton, C. S., Dufresne, J. L., Hall, A., Hallegatte, S., Holland, M. M., Ingram, W., Randall, D. A., Soden, B. J., Tselioudis, G., & Webb, M. J. (2006). How well do we understand and evaluate climate change feedback processes? *Journal of Climate*, 19, 3445–3482. https://doi.org/10.1175/JCLI3819.1

Bowman, K. W., Cressie, N., Qu, X., & Hall, A. (2018). A Hierarchical Statistical Framework for Emergent Constraints: Application to Snow-Albedo Feedback. *Geophysical Research Letters*, 45(23), 13,050-13,059. https://doi.org/10.1029/2018GL080082

Brient, F., & Schneider, T. (2016). Constraints on climate sensitivity from space-based measurements of low-cloud reflection. *Journal of Climate*, 29(16), 5821–5835. https://doi.org/10.1175/JCLI-D-15-0897.1

Brient, F., Schneider, T., Tan, Z., Bony, S., Qu, X., & Hall, A. (2016). Shallowness of tropical low clouds as a predictor of climate models’ response to warming. *Climate Dynamics*, 47(1–2), 433–449. https://doi.org/10.1007/s00382-015-2846-0

Caldwell, P. M., Bretherton, C. S., Zelinka, M. D., Klein, S. A., Santer, B. D., & Sanderson, B. M. (2014). Statistical significance of climate sensitivity predictors obtained by data mining. *Geophysical Research Letters*, 41(5), 1803–1808. https://doi.org/10.1002/2014GL059205

Caldwell, P. M., Zelinka, M. D., & Klein, S. A. (2018). Evaluating emergent constraints on equilibrium climate sensitivity. *Journal of Climate*, 31(10), 3921–3942. https://doi.org/10.1175/JCLI-D-17-0631.1

Caldwell, P. M., Zelinka, M. D., Taylor, K. E., & Marvel, K. (2016). Quantifying the sources of intermodel spread in equilibrium climate sensitivity. *Journal of Climate*, 29(2), 513–524. https://doi.org/10.1175/JCLI-D-15-0352.1

Cesana, G. v., & del Genio, A. D. (2021). Observational constraint on cloud feedbacks suggests moderate climate sensitivity. *Nature Climate Change*, 11(3), 213–218. https://doi.org/10.1038/s41558-020-00970-y

Cess, R. D., Potter, G. L., Blanchet, J. P., Boer, G. J., Genio, A. D. D., D É Qu É, M., Dymnikov, V., Galin, V., Gates, W. L., Ghan, S. J., Kiehl, J. T., Lacis, A. A., Treut, H. le, Li, Z. X., Liang, X. Z., Mc Avaney, B. J., Meleshko, V. P., Mitchell, J. F. B., Morcrette, J. J., … Zhang, M. H. (1990). Intercomparison and interpretation of climate feedback processes in 19 atmospheric general circulation models. *Journal of Geophysical Research*, 95(D10). https://doi.org/10.1029/jd095id10p16601

Eyring, V., Bony, S., Meehl, G. A., Senior, C. A., Stevens, B., Stouffer, R. J., & Taylor, K. E. (2016). Overview of the Coupled Model Intercomparison Project Phase 6 (CMIP6) experimental design and organization. *Geoscientific Model Development*, 9(5), 1937–1958. https://doi.org/10.5194/gmd-9-1937-2016

Forster, P., T. Storelvmo, K. Armour, W. Collins, J.-L. Dufresne, D. Frame, D.J. Lunt, T. Mauritsen, M.D. Palmer, M. Watanabe, M. Wild, and H. Zhang, The Earth's Energy Budget, Climate Feedbacks, and Climate Sensitivity. *In Climate Change 2021: The Physical Science Basis. Contribution of Working Group I to the Sixth Assessment Report of the Intergovernmental Panel on Climate Change* [Masson-Delmotte, V., P. Zhai, A. Pirani, S.L. Connors, C. Péan, S. Berger, N. Caud, Y. Chen, L. Goldfarb, M.I. Gomis, M. Huang, K. Leitzell, E. Lonnoy, J.B.R. Matthews, T.K. Maycock, T. Waterfield, O. Yelekçi, R. Yu, and B. Zhou (eds.)]. Cambridge University Press, Cambridge, United Kingdom and New York, NY, USA, 923–1054 (2021).

Gettelman, A., Hannay, C., Bacmeister, J. T., Neale, R. B., Pendergrass, A. G., Danabasoglu, G., Lamarque, J. -F., Fasullo, J. T., Bailey, D. A., Lawrence, D. M., & Mills, M. J. (2019). High Climate Sensitivity in the Community Earth System Model Version 2 (CESM2). *Geophysical Research Letters*, *46*(14), 8329–8337. https://doi.org/10.1029/2019gl083978

Grise, K. M., Polvani, L. M., & Fasullo, J. T. (2015). Reexamining the relationship between climate sensitivity and the Southern Hemisphere radiation budget in CMIP models. *Journal of Climate*, 28(23), 9298–9312. https://doi.org/10.1175/JCLI-D-15-0031.1

Hall, A., Cox, P., Huntingford, C., & Klein, S. (2019). Progressing emergent constraints on future climate change. *Nature Climate Change*, 9(4), 269–278. https://doi.org/10.1038/s41558-019-0436-6

Hersbach, H., Bell, B., Berrisford, P., Biavati, G., Horányi, A., Muñoz Sabater, J., Nicolas, J., Peubey, C., Radu, R., Rozum, I., Schepers, D., Simmons, A., Soci, C., Dee, D., Thépaut, J-N. (2023). ERA5 monthly averaged data on single levels from 1940 to present. Copernicus Climate Change Service (C3S) Climate Data Store (CDS) [Dataset]. https://doi.org/10.24381/cds.f17050d7

Hersbach, H., Bell, B., Berrisford, P., Hirahara, S., Horányi, A., Muñoz-Sabater, J., Nicolas, J., Peubey, C., Radu, R., Schepers, D., Simmons, A., Soci, C., Abdalla, S., Abellan, X., Balsamo, G., Bechtold, P., Biavati, G., Bidlot, J., Bonavita, M., … Thépaut, J. N. (2020). The ERA5 global reanalysis. *Quarterly Journal of the Royal Meteorological Society*, 146(730), 1999–2049. https://doi.org/10.1002/qj.3803

Hirota, N., Ogura, T., Shiogama, H., Caldwell, P., Watanabe, M., Kamae, Y., & Suzuki, K. (2021). Underestimated marine stratocumulus cloud feedback associated with overly active deep convection in models. *Environmental Research Letters*, 16(7). https://doi.org/10.1088/1748-9326/abfb9e

Jiang, X., Su, H., Jiang, J. H., Neelin, J. D., Wu, L., Tsushima, Y., & Elsaesser, G. (2023). Muted extratropical low cloud seasonal cycle is closely linked to underestimated climate sensitivity in models. *Nature Communications*, 14(5586). https://doi.org/10.1038/s41467-023-41360-0

Kang, S. M., Ceppi, P., Yu, Y., & Kang, I. S. (2023). Recent global climate feedback controlled by Southern Ocean cooling. *Nature Geoscience*, 16(9), 775–780. https://doi.org/10.1038/s41561-023-01256-6

Kang, S. M., Hawcroft, M., Xiang, B., Hwang, Y. T., Cazes, G., Codron, F., Crueger, T., Deser, C., Hodnebrog, Ø., Kim, H., Kim, J., Kosaka, Y., Losada, T., Mechoso, C. R., Myhre, G., Seland, Ø., Stevens, B., Watanabe, M., & Yu, S. (2019). Extratropical–tropical interaction model intercomparison project (ETIN-MIP): Protocol and initial results. *Bulletin of the American Meteorological Society*, 100(12), 2589–2605. https://doi.org/10.1175/BAMS-D-18-0301.1

Kang, S. M., Xie, S.-P., Shin, Y., Kim, H., Hwang, Y.-T., Stuecker, M. F., Xiang, B., & Hawcroft, M. (2020). Walker circulation response to extratropical radiative forcing. *Science Advances*, 6.

Kato, S., Rose, F. G., Rutan, D. A., Thorsen, T. J., Loeb, N. G., Doelling, D. R., Huang, X., Smith, W. L., Su, W., & Ham, S. H. (2018). Surface irradiances of edition 4.0 Clouds and the Earth’s Radiant Energy System (CERES) Energy Balanced and Filled (EBAF) data product. *Journal of Climate*, 31(11), 4501–4527. https://doi.org/10.1175/JCLI-D-17-0523.1

Kay, J. E., Bourdages, L., Miller, N. B., Morrison, A., Yettella, V., Chepfer, H., & Eaton, B. (2016). Evaluating and improving cloud phase in the Community Atmosphere Model version 5 using spaceborne lidar observations. *Journal of Geophysical Research: Atmospheres*, 1–19. https://doi.org/10.1002/2014JD022994.Received

Klein, S. A., & Hall, A. (2015). Emergent Constraints for Cloud Feedbacks. *Current Climate Change Reports*, 1(4), 276–287. https://doi.org/10.1007/s40641-015-0027-1

Klein, S. A., Zhang, Y., Zelinka, M. D., Pincus, R., Boyle, J., & Gleckler, P. J. (2013). Are climate model simulations of clouds improving? An evaluation using the ISCCP simulator. *Journal of Geophysical Research Atmospheres*, 118(3), 1329–1342. https://doi.org/10.1002/jgrd.50141

Lauer, A., Bock, L., Hassler, B., Schröder, M., & Stengel, M. (2023). Cloud Climatologies from Global Climate Models-A Comparison of CMIP5 and CMIP6 Models with Satellite Data. *Journal of Climate*, *36*(2), 281–311. https://doi.org/10.1175/JCLI-D-22-0181.1

Lauer, A., & Hamilton, K. (2013). Simulating clouds with global climate models: A comparison of CMIP5 results with CMIP3 and satellite data. *Journal of Climate*, *26*(11), 3823–3845. https://doi.org/10.1175/JCLI-D-12-00451.1

Lipat, B. R., Tselioudis, G., Grise, K. M., & Polvani, L. M. (2017). CMIP5 models' shortwave cloud radiative response and climate sensitivity linked to the climatological Hadley cell extent. *Geophysical Research Letters*, 44(11), 5739–5748. https://doi.org/10.1002/2017GL073151

Loeb, N. G., Doelling, D. R., Wang, H., Su, W., Nguyen, C., Corbett, J. G., Liang, L., Mitrescu, C., Rose, F. G., & Kato, S. (2018). Clouds and the Earth's Radiant Energy System (CERES) Energy Balanced and Filled (EBAF) top-of-atmosphere (TOA) edition-4.0 data product. *Journal of Climate*, 31(2), 895–918. https://doi.org/10.1175/JCLI-D-17-0208.1

Lutsko, N. J., Popp, M., Nazarian, R. H., & Albright, A. L. (2021). Emergent Constraints on Regional Cloud Feedbacks. *Geophysical Research Letters*, 48(10). https://doi.org/10.1029/2021GL092934

McCoy, D. T., Field, P., Bodas-Salcedo, A., Elsaesser, G. S., & Zelinka, M. D. (2020). A Regime-Oriented Approach to Observationally Constraining Extratropical Shortwave Cloud Feedbacks. *Journal of Climate*, 33(23), 9967–9983. https://doi.org/10.1175/jcli-d-19-0987.1

McCoy, D. T., Tan, I., Hartmann, D. L., Zelinka, M. D., & Storelvmo, T. (2016). On the relationships among cloud cover, mixed-phase partitioning, and planetary albedo in GCMs. *Journal of Advances in Modeling Earth Systems*, 8(2), 650–668. https://doi.org/10.1002/2015MS000589

Mechoso, C. R., Losada, T., Koseki, S., Mohino-Harris, E., Keenlyside, N., Castaño-Tierno, A., Myers, T. A., Rodriguez-Fonseca, B., & Toniazzo, T. (2016). Can reducing the incoming energy flux over the Southern Ocean in a CGCM improve its simulation of tropical climate? *Geophysical Research Letters*, 43(20), 11,057-11,063. https://doi.org/10.1002/2016GL071150

Meehl, G. A., Covey, C., Delworth, T., Latif, M., McAvaney, B., Mitchell, J. F. B., Stouffer, R. J., & Taylor, K. E. (2007). The WCRP CMIP3 multimodel dataset: A new era in climatic change research. *Bulletin of the American Meteorological Society*, 88(9), 1383–1394. https://doi.org/10.1175/BAMS-88-9-1383

Myers, T. A., & Norris, J. R. (2016). Reducing the uncertainty in subtropical cloud feedback. Geophysical Research Letters, 43(5), 2144–2148. https://doi.org/10.1002/2015GL067416

Myers, T. A., Scott, R. C., Zelinka, M. D., Klein, S. A., Norris, J. R., & Caldwell, P. M. (2021). Observational constraints on low cloud feedback reduce uncertainty of climate sensitivity. *Nature Climate Change*, 11(6), 501–507. https://doi.org/10.1038/s41558-021-01039-0

Nam, C., Bony, S., Dufresne, J. L., & Chepfer, H. (2012). The too few, too bright tropical low-cloud problem in CMIP5 models. *Geophysical Research Letters*, *39*(21). https://doi.org/10.1029/2012GL053421

Qu, X., Hall, A., Klein, S. A., & Caldwell, P. M. (2014). On the spread of changes in marine low cloud cover in climate model simulations of the 21st century. *Climate Dynamics*, 42(9–10), 2603–2626. https://doi.org/10.1007/s00382-013-1945-z

Qu, X., Hall, A., Klein, S. A., & Deangelis, A. M. (2015). Positive tropical marine low-cloud cover feedback inferred from cloud-controlling factors. *Geophysical Research Letters*, 42(18), 7767–7775. https://doi.org/10.1002/2015GL065627

Schlund, M., Lauer, A., Gentine, P., Sherwood, S. C., & Eyring, V. (2020). Emergent constraints on equilibrium climate sensitivity in CMIP5: Do they hold for CMIP6? *Earth System Dynamics*, 11(4), 1233–1258. https://doi.org/10.5194/esd-11-1233-2020

Shell, K. M., Kiehl, J. T., & Shields, C. a. (2008). Using the radiative kernel technique to calculate climate feedbacks in NCAR's Community Atmospheric Model. *Journal of Climate*, 21, 2269–2282. https://doi.org/10.1175/2007JCLI2044.1

Sherwood, S., Webb, M. J., Annan, J. D., Armour, K. C., Forster, P. M., Hargreaves, J. C., Hegerl, G., Klein, S. A., Marvel, K. D., Rohling, E. J., Watanabe, M., Andrews, T., Braconnot, P., Bretherton, C. S., Foster, G. L., Hausfather, Z., Heydt, A. S. von der, Knutti, R., Mauritsen, T., … Zelinka, M. D. (2020). An assessment of Earth's climate sensitivity using multiple lines of evidence. *Reviews of Geophysics*, 58, e2019RG000678. https://doi.org/10.1029/2019RG000678

Siler, N., Po-Chedley, S., & Bretherton, C. S. (2018). Variability in modeled cloud feedback tied to differences in the climatological spatial pattern of clouds. *Climate Dynamics*, 50(3–4), 1209–1220. https://doi.org/10.1007/s00382-017-3673-2

Soden, B. J., Held, I. M., Colman, R. C., Shell, K. M., Kiehl, J. T., & Shields, C. a. (2008). Quantifying climate feedbacks using radiative kernels. *Journal of Climate*, 21(1988), 3504–3520. https://doi.org/10.1175/2007JCLI2110.1

Taylor, K. E., Stouffer, R. J., & Meehl, G. A. (2012). An Overview of CMIP5 and the Experiment Design. *Bulletin of the American Meteorological Society*, 3(April), 485–498. https://doi.org/10.1175/BAMS-D-11-00094.1

Terai, C. R., Klein, S. A., & Zelinka, M. D. (2016). Constraining the low-cloud optical depth feedback at middle and high latitudes using satellite observations. *Journal of Geophysical Research*, 121(16), 9696–9716. https://doi.org/10.1002/2016JD025233

Thackeray, C. W. (2024). cwthackeray/GRL-clouds: Thackeray24 (Version 1.0.0) [Software]. Zenodo. https://doi.org/10.5281/zenodo.14226936

Tian, B. (2015). Spread of model climate sensitivity linked to double-Intertropical Convergence Zone bias. *Geophysical Research Letters*, *42*(10), 4133–4141. https://doi.org/10.1002/2015GL064119

Trenberth, K. E., & Fasullo, J. T. (2010). Simulation of present-day and twenty-first-century energy budgets of the southern oceans. *Journal of Climate*, 23(2), 440–454. https://doi.org/10.1175/2009JCLI3152.1

Vignesh, P. P., Jiang, J. H., Kishore, P., Su, H., Smay, T., Brighton, N., & Velicogna, I. (2020). Assessment of CMIP6 Cloud Fraction and Comparison with Satellite Observations. *Earth and Space Science*, *7*(2). https://doi.org/10.1029/2019EA000975

Volodin, E. M. (2008). Relation between temperature sensitivity to doubled carbon dioxide and the distribution of clouds in current climate models. *Izvestiya, Atmospheric and Oceanic Physics*, 44(3), 288–299. https://doi.org/10.1134/S0001433808030043

Wall, C. J., Storelvmo, T., Norris, J. R., & Tan, I. (2022). Observational Constraints on Southern Ocean Cloud-Phase Feedback. *Journal of Climate*, 35, 5087–5102. https://doi.org/10.1175/JCLI-D-21

Webb, M. J., Lambert, F. H., & Gregory, J. M. (2013). Origins of differences in climate sensitivity, forcing and feedback in climate models. *Climate Dynamics*, 40(3–4), 677–707. https://doi.org/10.1007/s00382-012-1336-x

Webb, M. J., & Lock, A. P. (2020). Testing a Physical Hypothesis for the Relationship Between Climate Sensitivity and Double-ITCZ Bias in Climate Models. *Journal of Advances in Modeling Earth Systems*, *12*. https://doi.org/10.1029/2019MS001999

Williams, K. D., & Tselioudis, G. (2007). GCM intercomparison of global cloud regimes: Present-day evaluation and climate change response. *Climate Dynamics*, 29(2–3), 231–250. https://doi.org/10.1007/s00382-007-0232-2

Williamson, M. S., Thackeray, C. W., Cox, P. M., Hall, A., Huntingford, C., & Nijsse, F. J. M. M. (2021). Emergent constraints on climate sensitivities. *Reviews of Modern Physics*, 93(2), 025004. https://doi.org/10.1103/RevModPhys.93.025004

Zelinka, M. D., Myers, T. A., McCoy, D. T., Po-Chedley, S., Caldwell, P. M., Ceppi, P., Klein, S. A., & Taylor, K. E. (2020). Causes of Higher Climate Sensitivity in CMIP6 Models. *Geophysical Research Letters*, 47(1), e2019GL085782. https://doi.org/10.1029/2019GL085782

Zhai, C., Jiang, J. H., & Su, H. (2015). Long-term cloud change imprinted in seasonal cloud variation: More evidence of high climate sensitivity. *Geophysical Research Letters*, 42(20), 8729–8737. https://doi.org/10.1002/2015GL065911

Zhou, C., Zelinka, M. D., Dessler, A. E., & Klein, S. A. (2015). The relationship between interannual and long-term cloud feedbacks. *Geophysical Research Letters*, 42(23), 10463–10469. https://doi.org/10.1002/2015GL066698

Zhou, W., Leung, L. R., Siler, N., & Lu, J. (2023). Future precipitation increase constrained by climatological pattern of cloud effect. *Nature Communications*, *14*(1), 6363. https://doi.org/10.1038/s41467-023-42181-x

Zhu, J., Otto-Bliesner, B. L., Brady, E. C., Gettelman, A., Bacmeister, J. T., Neale, R. B., Poulsen, C. J., Shaw, J. K., McGraw, Z. S., & Kay, J. E. (2022). LGM Paleoclimate Constraints Inform Cloud Parameterizations and Equilibrium Climate Sensitivity in CESM2. *Journal of Advances in Modeling Earth Systems*, *14*(4). https://doi.org/10.1029/2021MS002776